FLOW STATE TRANSITION OF MIXED CONVECTION IN VERTICAL CHANNEL WITH HORIZONTAL PRESSURE GRADIENT

Yuki Matsukawa, Ryo Araki and Takahiro Tsukahara
Department of Mechanical and Aerospace Engineering
Tokyo University of Science
2641 Yamazaki, Noda-shi, Chiba 278-8510, Japan
7523701@ed.tus.ac.jp, araki.ryo@rs.tus.ac.jp, tsuka@rs.tus.ac.jp

ABSTRACT

In forced convection of wall-bounded shear flows, those subcritical transition processes exhibit intermittent structures, e.g., turbulent stripes or puffs), with spatiotemporal intermittency. In this study, we performed direct numerical simulations of mixed convection in a vertical channel with a horizontal pressure gradient. We discovered that the horizontal flow at moderate Reynolds numbers cancels out the instability of roll cells in the vertical natural convection. We draw a flow map in a phase space of the Rayleigh number and friction Reynolds number, which are relevant to the vertical and horizontal flows, respectively.

INTRODUCTION

There are supercritical and subcritical transitions in the turbulent transition process of fluid flow. In the supercritical transition, when the Reynolds number *Re* exceeds a linear stability (local stability) critical Reynolds number (Re_{L}), the base flow becomes unstable and moves to a different stable steady solution. After that, each time the Reynolds number reaches a critical value, the flow becomes progressively more complex, eventually leading to turbulence. For example, the Rayleigh–Bénard convection and the Taylor–Couette flow are typical flow systems that undergo a supercritical transition. On the other hand, subcritical transitions are those in which laminar and turbulent flows coexist below Re_{L} and have spatiotemporal intermittency (Tuckerman *et al.*, 2020). These turbulent intermittent structures are maintained until the global stability critical Reynolds number (Re_{G}) and are called turbulent stripes or puffs. In the subcritical transition region accompanied by the intermittent structures, the Nusselt number *Nu* is close to the value estimated from empirical equations in turbulent regions (Fukuda & Tsukahara, 2020), implying the practical importance of such subcritical transition studies from the viewpoint of improving heat transfer efficiency.

The mixed convection in vertical channel flow (MCVCF) is a combination of plane Poiseuille flow (PPF) and vertical channel flow (VCF), as described below, and horizontal Poiseuille flow (pressure gradient driven) is provided orthogonally to the vertical buoyancy-induced natural convection. The flow field in which forced convection and natural convection are combined is called mixed convection (or combined convection), and most of the forced convection on the ground is strictly mixed convection. Although forced convection without the influence of natural convection is an idealized system of the real flow field, it is highly important to study mixed convection, which is ubiquitous in the real system.

The PPF is a system in which the pressure gradient between two parallel plates drives the fluid, and Re_{L} is $Re_{\mathrm{c}} = 5772$ according to the linear stability theory (based on the channel center velocity u_{c}, channel half-width δ and kinematic viscosity ν) (Orszag, 1971). The turbulent stripe structure develops in the subcritical transition region (Tsukahara *et al.*, 2005). On the other hand, VCF is a natural convection flow originating from the density difference between two parallel plates with different temperatures. Thermal convection systems such as VCF usually undergo a supercritical turbulent transition process, and the first critical Rayleigh number at which a two-dimensional roll cell structure appears is determined to be $Ra_{\mathrm{cr1}} = 5708$ (Bergholz, 1978; Ruth, 1979; Gao *et al.*, 2013). In the “subcritical” region below the second critical value of $Ra_{\mathrm{cr2}} \approx 10200$, where a secondary instability occurs, the three-dimensional flow field resembles the turbulent stripes often seen in the forced convection, where the Rayleigh number is gradually reduced from turbulent to laminar flow in a so-called reverse transition condition, and a series of horizontal vortices form stripes. In this study, we investigated the quantitative contribution of these two orthogonal flow components to the transitional states and heat transfer efficiency using direct numerical simulations (DNSs).

PROBLEM SETUP

The analysis target is an MCVCF, as shown in Fig. 1, in which vertical natural convection and horizontal pressure gradient-driven flow are induced simultaneously between two parallel plates. The velocity boundary condition is the no-slip condition on the wall surface, and the temperature boundary condition is the constant temperature difference between the hot wall T_{h} and the cold wall T_{c}, $\Delta T = T_{\mathrm{h}} - T_{\mathrm{c}}$. The working fluid is an incompressible Newtonian fluid with constant properties using the Boussinesq approximation. We performed DNSs in order to reproduce turbulent phenomena accurately. The governing equations are the continuity equation, Navier–Stokes equation, and the energy equation:

$$\frac{\partial u_i^*}{\partial x_i^*} = 0, \tag{1}$$

$$\frac{\partial u^*}{\partial t^*} + u_i^* \frac{\partial u^*}{\partial x_i^*} = -\frac{\partial p^*}{\partial x^*} + Pr \frac{\partial^2 u^*}{\partial x_i^* \partial x_i^*} - \frac{\mathrm{d}P^*}{\mathrm{d}x^*}, \tag{2}$$

$$\frac{\partial v^*}{\partial t^*} + u_i^* \frac{\partial v^*}{\partial x_i^*} = -\frac{\partial p^*}{\partial y^*} + Pr \frac{\partial^2 v^*}{\partial x_i^* \partial x_i^*}, \tag{3}$$

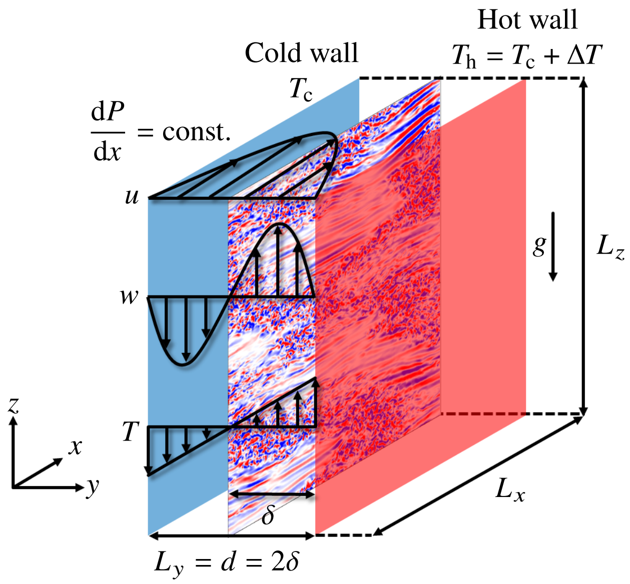

Figure 1 Configuration of Mixed Convection in Vertical Channel Flow (MCVCF). The schematic profiles of u, w, and T represent the laminar solutions. The color contour shows a snapshot of wall-normal velocity distribution in the gap center plane, obtained by a present DNS at moderate Ra and $Re_{\tau,x}$.

Table 1 Numerical conditions of MCVCF: L_i, the domain length; N_i, the number of grids. Δi_x^+ and Δi_z^+ are the grid resolutions in the x and z wall unit.

$Re_{\tau,x}$	0, 30, 40, 60, 80				
Ra	5600	5800	6000	6200	6600
Pr	0.71				
Ri (except for $Re_{\tau,x=0}$ case)	0.022	0.023	0.024	0.024	0.026
$L_x \times L_y \times L_z$	$51.2d \times d \times 51.2d$				
$N_x \times N_y \times N_z$	$1024 \times 128 \times 1024$				
$\Delta x_x^+, \Delta x_z^+$	≤ 8.01				
$\Delta y_x^+, \Delta y_z^+$	≤ 2.23				
$\Delta z_x^+, \Delta z_z^+$	≤ 8.01				

$$\frac{\partial w^*}{\partial t^*} + u_i^* \frac{\partial w^*}{\partial x_i^*} = -\frac{\partial p^*}{\partial z^*} + Pr \frac{\partial^2 w^*}{\partial x_i^* \partial x_i^*} + RaPr\theta, \quad (4)$$

$$\frac{\partial \theta}{\partial t^*} + u_i^* \frac{\partial \theta}{\partial x_i^*} = \frac{\partial^2 \theta}{\partial x_i^* \partial x_i^*}. \quad (5)$$

The last term in Eq. (2) is an external force term with constant mean pressure gradient ($\mathrm{d}P^*/\mathrm{d}x^* = $ const.) where the superscript $(\quad)^*$ denotes dimensionless due to the channel width d (or 2δ) and the thermal diffusion coefficient α. Since no physical quantity corresponds to the representative velocity in the DNS code under analysis, which is based on the VCF, the code is non-dimensionalized, as in Eq. (6).

$$\mathbf{x}^* = \frac{\mathbf{x}}{d}, \quad \mathbf{u}^* = \frac{\mathbf{u}}{\alpha/d}, \quad p^* = \frac{p}{\rho(\alpha/d)^2}, \quad t^* = \frac{t}{d^2/\alpha},$$
$$\theta = \frac{T - T_\mathrm{ref}}{\Delta T}, \quad \text{where } T_\mathrm{ref} = \frac{T_\mathrm{h} + T_\mathrm{c}}{2}. \quad (6)$$

The control parameters are defined by Eq. (7): Rayleigh number Ra, Prandtl number $Pr\,(=0.71)$, and friction Reynolds number in the x direction $Re_{\tau,x}$.

$$Ra = \frac{g\beta\Delta T d^3}{\nu\alpha}, \; Pr = \frac{\nu}{\alpha}, \; Re_{\tau,x} = \frac{u_\tau \delta}{\nu} = \sqrt{-\frac{1}{8Pr^2}\frac{\mathrm{d}P^*}{\mathrm{d}x^*}} \quad (7)$$

In Eq. (7), β is the coefficient of thermal expansion. As shown in Table 1, to capture the expected large-scale intermittent structure, a long computational domain with a periodic boundary was provided in the x and z directions. The friction Reynolds number in the x direction for each Rayleigh number was set to $Re_{\tau,x} = 0$–80. The Rayleigh number Ra is set to be between $Ra_\mathrm{cr1} = 5708$ and $Ra_\mathrm{cr2} = 10200$ (subcritical to the second critical value). The Richardson number Ri in Table 1 represents the ratio of natural to forced convection defined as $Ri = Gr/Re_{\mathrm{m},x}^2$ ($Gr = g\beta\Delta T d^3/\nu^2$: Grashof number, $Re_{\mathrm{m},x} = u_\mathrm{m} d/\nu$: bulk Reynolds number in x direction). We list the maximum value of Ri in Table 1 for $Re_{\tau,x} \neq 0$, since

$Ri \to \infty$ when $Re_{\tau,x} \to 0$. For $Ri \gg 1$, the natural convection dominates; for $Ri \approx 1$, the two compete; and for $Ri \ll 1$, the forced convection dominates. Thus, the flow field is dominated by the forced convection in all cases where $Re_{\tau,x} \neq 0$. In these simulations, the initial field was a turbulent flow field, and the flow field was created by quasi-static reduction of the Rayleigh number toward a given value (that is, reverse transition).

RESULTS AND DISCUSSIONS

Figure 2 shows the flow state transition diagram of the flow field by taking Ra on the vertical axis and $Re_{\tau,x}$ on the horizontal axis. The newly investigated region in this study is for $Re_{\tau,x} \geq 30$, and for $Re_{\tau,x} = 30$ and 40, the two-dimensional roll cell structures seen for $(Re_{\tau,x}, Ra) = (0, 5800)$ appear in all cases except for $(Re_{\tau,x}, Ra) = (30, 5600)$ and $(40, 5600)$. In the cases of $(Re_{\tau,x}, Ra) = (30, 5600)$ and $(40, 5600)$, complete laminar flow fields were observed as in the case of $(Re_{\tau,x}, Ra) = (0, 5600)$. Furthermore, when the forced convection component is enhanced and $Re_{\tau,x}(= 60$ and $80)$ exceeds the global stability critical Reynolds number Re_{G} of the PPF, turbulent stripe structures similar to that seen in forced convection appears for all conditions. It is noteworthy that although a three-dimensional flow structure appears at $(Re_{\tau,x}, Ra) = (0, 6000\text{–}6600)$, the instability is once suppressed as $Re_{\tau,x}$ increases from 0. Further increased $Re_{\tau,x}$ leads an onset of a two-dimensional roll cell structure, the flow field becomes unstable again and turbulent stripes originating from forced convection appear. This means that the horizontal instability, which should have been caused by the natural convection component at $Ra \geq 6000$, is mitigated by the addition of the horizontal forced convection component. Such a stabilization phenomenon at moderate Reynolds numbers was also observed in the transition phenomenon of the Taylor–Couette–Poiseuille flow (TCPF) described in our previous paper (Matsukawa & Tsukahara, 2023)—TCPF is a combined shear annular pipe flow that consists of azimuthal Couette flow and axial Poiseuille flow. The flow field was stabilized to a complete laminar flow at moderate Reynolds number, and no turbulent flow or roll cell structure was observed. The two-dimensional roll cell structure, which is the primely unstable base flow with $Ra > 5708 = Ra_{\mathrm{cr1}}$, is caused by the vertical instability, and the second instability on the roll cells might be avoided by an interference from the horizontal forced convection component and that is why it did not lead to a complete laminar flow. Both MCVCF and TCPF are combined shear flows with multiple orthogonal shears, suggesting that stabilization of the flow field occurs at moderate Reynolds numbers in such flow fields.

Figure 2 shows the Nusselt number Nu obtained from our DNSs. The horizontal axis is Ra, and the increasing trend of Nu for each $Re_{\tau,x}$ is summarized. For $Re_{\tau,x} = 0$–40, Nu increases linearly with increasing Ra, although the slope differs. Compared to previous studies (Gao *et al.*, 2013; Cimarelli & Angeli, 2017) for pure-VCF with no forced convection component ($Re_{\tau,x} = 0$), the present DNS shows higher Nu for $Re_{\tau,x} = 0$. This is because the computational domain has been enlarged to capture more global structures. The addition of the horizontal forced convection component stabilizes the flow structure at $Re_{\tau,x} = 30$ and 40, but the heat transfer efficiency is generally higher than that at $Re_{\tau,x} = 0$. However, there is no significant difference in Nu between $Re_{\tau,x} = 30$ and 40. For $Re_{\tau,x} = 60$ and 80, where the turbulent stripes appear due to forced convection, $Nu \approx 1.8$ and 2.6, respectively, which are significantly different values, indicating more enhanced heat transfer.

CONCLUSIONS

In this study, we performed DNSs for the subcritical transition phenomena of mixed convection in vertical channel flow (MCVCF). For all Ra conditions, the turbulent stripe structure appeared in $Re_{\tau,x} \geq 60$ because the value of $Re_{\tau,x}$ exceeded the Re_{G} of the PPF. However, in the process leading to the appearance of turbulent stripes, two-dimensional roll cell structures appeared at $Re_{\tau,x} = 30$ and 40, even when three-dimensional structures derived from natural convection appeared at $Re_{\tau,x} = 0$. The horizontal instability caused by the natural convection component is mitigated by the horizontally given forced convection component, resulting in a stabilization of the second instability of roll cells as found in other combined shear flows such as TCPF. In addition, high heat transfer characteristics can be obtained by providing forced convection in the horizontal direction.

ACKNOWLEDGEMENTS

This work was supported by a Grant-in-Aid for the Japan Society for the Promotion of Science (JSPS) Fellowship 19H02071. Direct numerical simulations were performed on SX-series supercomputers at the Cybermedia Center of Osaka University and the Cyberscience Center of Tohoku University. We also greatly appreciate the cooperation of Mr. Shun Onodera, a graduate of Tokyo University of Science.

REFERENCES

Bergholz, R. F. 1978 Instability of steady natural convection in a vertical fluid layer. *Journal of Fluid Mechanics* **84** (4), 743–768.

Cimarelli, A. & Angeli, D. 2017 Routes to chaos of natural convection flows in vertical channels. *International Communications in Heat and Mass Transfer* **81**, 201–209.

Fukuda, T. & Tsukahara, T. 2020 Heat transfer of transitional regime with helical turbulence in annular flow. *International Journal of Heat and Fluid Flow* **82**, 108555.

Gao, Z., Sergent, A., Podvin, B., Xin, S., Patrick, L. Q. & Tuckerman, L. S. 2013 Transition to chaos of natural convection between two infinite differentially heated vertical plates. *Physical Review E* **88**, 023010.

Matsukawa, Y. & Tsukahara, T. 2023 Parameter dependence of switching between supercritical and subcritical turbulent transitions in inner-cylinder rotating Taylor–Couette–Poiseuille flow. In *Proceedings of 10th International Symposium on Turbulence, Heat and Mass Transfer*.

Orszag, S. A. 1971 Accurate solution of the Orr–Sommerfeld stability equation. *Journal of Fluid Mechanics* **50** (4), 689–703.

Ruth, D. W. 1979 On the transition to transverse rolls in an infinite vertical fluid layer—A power series solution. *International Journal of Heat and Mass Transfer* **22** (8), 1199–1208.

Tsukahara, T., Seki, Y., Kawamura, H. & Tochio, D. 2005 DNS of turbulent channel flow at very low Reynolds numbers. In *Proceedings of 4th International Symposium on Turbulence and Shear Flow Phenomena*, pp. 935–940.

Tuckerman, L. S., Chantry, M. & Barkley, D. 2020 Patterns in Wall-Bounded Shear Flows. *Annual Review of Fluid Mechanics* **52** (1), 343–367.

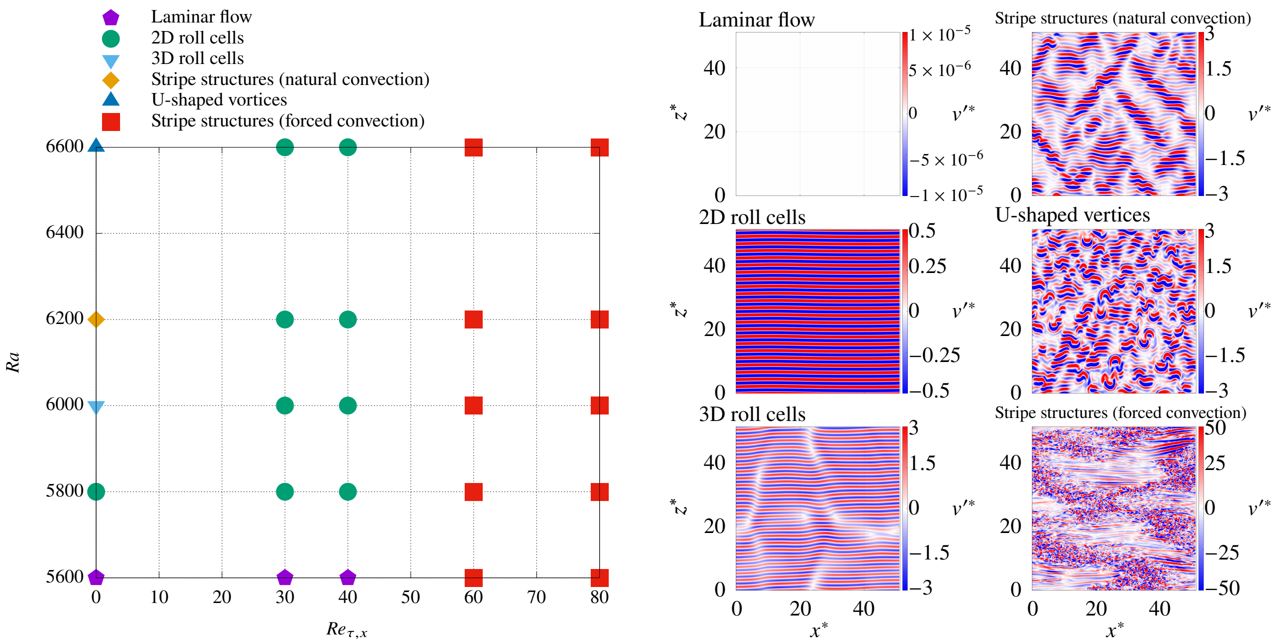

Figure 2 Flow state transition diagram of MCVCF for $Re_{\tau,x} = 0$–80, $Ra = 5600$–6600 and $Pr = 0.71$. The color contours show the wall-normal velocity distributions in the gap center plane: a wide green area corresponds to laminar, and regular horizontal blue and red streaks correspond to roll cells.

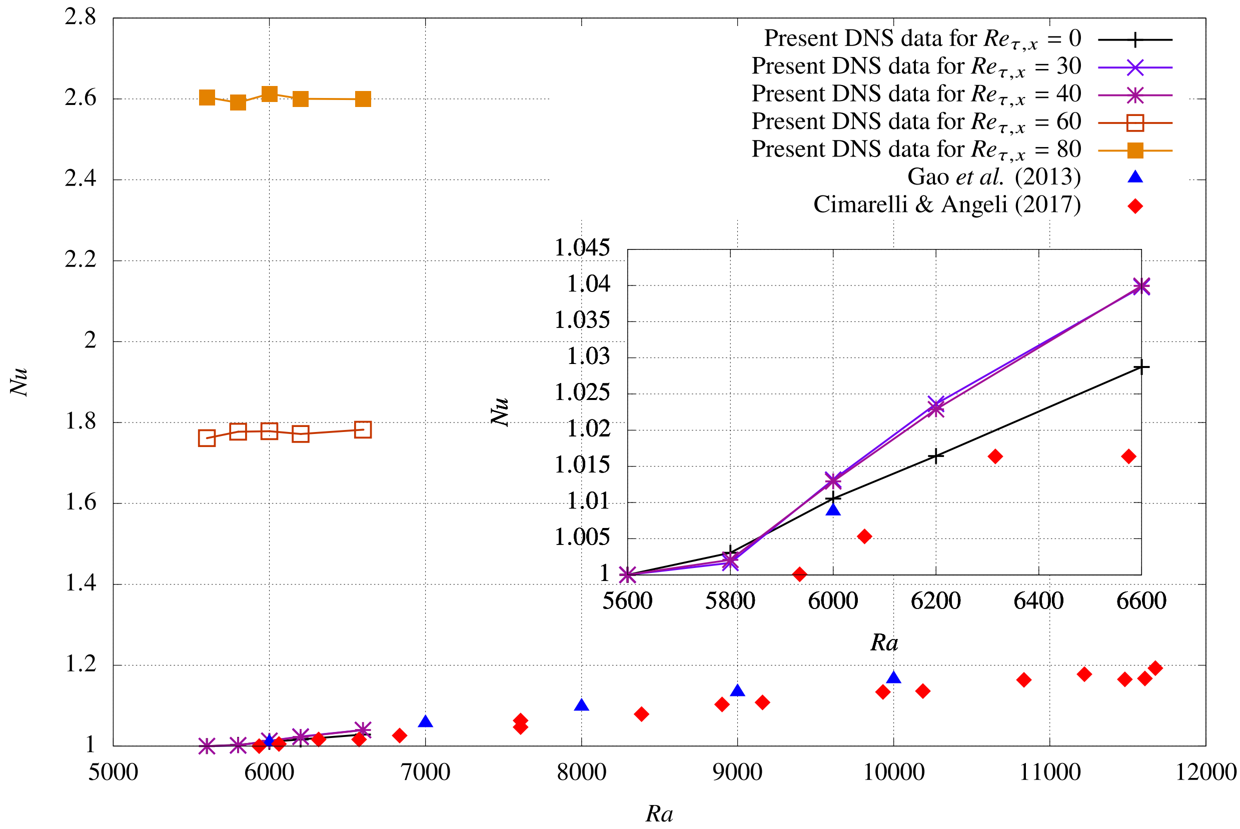

Figure 3 Nusselt number Nu versus Rayleigh number Ra of present DNS data for $Re_{\tau,x} = 0$–80. The filled triangle and square symbols are pure-VCF data ($Re_{\tau,x} = 0$) from Gao *et al.* (2013) and Cimarelli & Angeli (2017) respectively.